

Analytical expressions for z-scan with arbitrary phase change in thin nonlocal nonlinear media

A. Balbuena Ortega,^{1,*} M. L. Arroyo Carrasco,¹ M. M. Méndez Otero,¹ E. Reynoso Lara,² E. V. García Ramírez,³ and M. D. Iturbe Castillo⁴

¹Facultad de Ciencias Físico-Matemáticas, Benemérita Universidad Autónoma de Puebla, Av. San Claudio y 18 Sur. Col San Manuel, C.P. 72570, Puebla, Puebla, Mexico

²Facultad de Ciencias de la Electrónica, Benemérita Universidad Autónoma de Puebla, Av. San Claudio y 18 Sur. Col San Manuel, C.P. 72570, Puebla, Puebla, Mexico

³Instituto de Física, Universidad Nacional Autónoma de México, Circuito de la Investigación Científica Ciudad Universitaria CP. 04510 D. F., Mexico

⁴Instituto Nacional de Astrofísica, Óptica y Electrónica, Luis Enrique Erro # 1, C.P. 72840 Tonantzintla, Puebla, Mexico

*abalbuena1984@gmail.com

Abstract: Analytical expressions for the normalized transmittance of a thin material with simultaneous nonlocal nonlinear change in refraction and absorption are reported. Gaussian decomposition method was used to obtain the formulas that are adequate for any magnitude of the nonlinear changes. Particular cases of no locality are compared with the local case. Experimental results are reproduced (fitted) with the founded expressions.

©2014 Optical Society of America

OCIS codes: (190.0190) Nonlinear optics; (190.5940) Self-action effects.

References and links

1. M. Sheik-bahae, A. A. Said, and E. W. Van Stryland, "High-sensitivity, single-beam n_2 measurements," *Opt. Lett.* **14**(17), 955–957 (1989).
2. M. Sheik-Bahae, A. A. Said, T. H. Wei, D. J. Hagan, and E. W. Van Stryland, "Sensitive measurement of optical nonlinearities using a single beam," *IEEE J. Quantum Electron.* **26**(4), 760–769 (1990).
3. D. Weaire, B. S. Wherrett, D. A. B. Miller, and S. D. Smith, "Effect of low-power nonlinear refraction on laser-beam propagation in InSb," *Opt. Lett.* **4**(10), 331–333 (1979).
4. S. Hughes and B. S. Wherrett, "Fast Fourier Transform techniques for efficient simulation of z-scan measurements," *J. Opt. Soc. Am. B* **12**(10), 1888–1893 (1995).
5. R. E. Samad and N. D. Viera, "Analytical description of z-scan on-axis intensity based on the Huygens-Fresnel principle," *J. Opt. Soc. Am. B* **15**(11), 2742–2747 (1998).
6. B. Yao, L. Ren, and X. Hou, "Z-scan theory based on a diffraction model," *J. Opt. Soc. Am. B* **20**(6), 1290–1294 (2003).
7. G. Tsigaridas, M. Fakis, I. Polyzos, M. Tsibouri, P. Persephonis, and V. Giannetas, "Z-scan analysis for near-Gaussian beams through Hermite-Gaussian decomposition," *J. Opt. Soc. Am. B* **20**(4), 670–676 (2003).
8. L. Pálfalvi, B. C. Tóth, G. Almási, J. A. Fülöp, and J. Hebling, "A general Z-scan theory," *Appl. Phys. B* **97**(3), 679–685 (2009).
9. P. B. Chapple, J. Staromlynska, J. A. Hermann, T. J. McKay, and R. G. Mcduff, "Single-beam z-scan: measurement techniques and analysis," *Int. J. Nonlinear Opt. Phys.* **6**(03), 251–293 (1997).
10. S. Q. Chen, Z. B. Liu, W. P. Zang, J. G. Tian, W. Y. Zhou, F. Song, and C. P. Zhang, "Study on Z-scan characteristics for a large nonlinear phase shift," *J. Opt. Soc. Am. B* **22**(9), 1911–1916 (2005).
11. F. Q. Li, X. F. Zhang, F. Yang, N. Zong, Q. J. Peng, D. F. Cui, and Z. Y. Xu, "Analytical solution of on-axis beam propagation for z-scan technique," *J. Opt. Soc. Am. B* **26**(11), 2125–2130 (2009).
12. G. Tsigaridas, M. Fakis, I. Polyzos, P. Persephonis, and V. Giannetas, "Z-scan analysis for high order nonlinearities through Gaussian decomposition," *Opt. Commun.* **225**(4-6), 253–268 (2003).
13. B. Gu, J. Chen, Y. Fan, J. Ding, and H. T. Wang, "Study on Z-scan characteristics for a large nonlinear phase shift," *J. Opt. Soc. Am. B* **22**(9), 1911–1915 (2005).
14. B. Gu, K. Lou, J. Chen, H. T. Wang, and W. Ji, "Determination of the nonlinear refractive index in multiphoton absorbers by Z-scan measurements," *J. Opt. Soc. Am. B* **27**(11), 2438–2442 (2010).
15. E. V. García Ramírez, M. L. Arroyo Carrasco, M. M. Méndez Otero, E. Reynoso Lara, S. Chavez-Cerda, and M. D. Iturbe Castillo, "Z-scan and spatial self-phase modulation of a Gaussian beam in a thin nonlocal nonlinear media," *J. Opt.* **13**(8), 085203 (2011).

16. A. Balbuena Ortega, M. L. Arroyo Carrasco, M. M. Méndez Otero, V. L. Gayou, R. Delgado Macuil, H. Martínez Gutiérrez, and M. D. Iturbe Castillo, "Nonlocal nonlinear refractive index of gold nanoparticles synthesized by ascorbic acid reduction: comparison of fitting models," *J. Mod. Opt.* **61**(sup1), S68–S72 (2014).
17. J. A. Herman, "Beam propagation and optical power limiting with nonlinear media," *J. Opt. Soc. Am. B* **1**(5), 729–736 (1984).
18. E. V. Ramirez, M. L. Carrasco, M. M. Otero, S. C. Cerda, and M. D. Castillo, "Far field intensity distributions due to spatial self phase modulation of a Gaussian beam by a thin nonlocal nonlinear media," *Opt. Express* **18**(21), 22067–22079 (2010).
19. I. Mamedbeili and H. Nasibov, "Large third order optical nonlinearities in brilliant green solutions induced by CW He–Ne laser," *Laser Phys.* **19**(10), 2002–2007 (2009).

1. Introduction

The Z-scan technique, proposed by Sheik-Bahae et al. [1,2], is a widely used method to evaluate the real and imaginary parts of the nonlinear refractive index of optical materials. In this technique the far field intensity is measured as a function of the sample position. Two detection schemes are mainly used in this technique, one called closed aperture (to determine the nonlinear refraction) and the open aperture (to measure the nonlinear absorption). The transmittance, after a thin sample that is illuminated by a Gaussian beam, can be analytical calculated using different methods as: Gaussian decomposition (GD) [3], Fast Fourier Transform [4], Huygens-Fresnel principle [5], Kirchhoff-Fresnel diffraction theory [6], Hermite-Gauss decomposition [7], solving the paraxial wave equation [8], etc. GD analytical expressions for the normalized transmittance have been obtained for: weak nonlinearities in thin local Kerr media [2,9], high order refractive nonlinearities [5], large phase shifts [10]. Analytical expressions for the z-scan transmittance have also been obtained for large phase shifts using the Huygens-Fresnel principle [11]. However, numerical tools frequently require to obtain the normalized transmittance for nonlinear materials that present large refractive phase shifts [6,10], high order refractive nonlinearities [12] and for large nonlinear phase shifts with simultaneous third- and fifth-order refraction [13]. Influence of the multiphoton absorption process in a refractive Kerr media was analyzed by Gu et al. [14]. Recently a model to describe the z-scan curves for thin nonlocal nonlinear media with pure refractive nonlinearity was presented [15]. Based on such model experimental results have been adjusted, with a very good correspondence, for materials that present a purely refractive nonlinearity [15,16]. However, no analytical formulas for the z-scan transmittance have been proposed for thin nonlocal media with any magnitude of the nonlinear phase shift.

In this paper we obtain analytical formulas for the z-scan transmittance for thin materials that present a nonlocal refractive and absorptive nonlinearity. As in [15], an incident Gaussian beam was considered in order to calculate the output field after the sample, where the nonlocality of the material is taken into account through a single parameter m . GD was used to calculate the transmittance at far field and to obtain the analytical formulas without any restriction in the magnitude of the nonlinear phase shift. Z-scan curves for local and nonlocal special cases are compared. Experimental results of a material that present both nonlinear refraction and absorption are adjusted with the obtained formulas for a single value of m . Finally the conclusions are given.

2. Theoretical model

Consider a Gaussian beam propagating in the z direction with waist w_0 , wavelength λ , Rayleigh range $z_0 = \pi w_0^2 / \lambda$ and the following field amplitude:

$$E(r, z) = A_0 \frac{w_0}{w(z)} \exp \left[-\frac{r^2}{w(z)^2} \right] \exp \left[-ikz - ik \frac{r^2}{2R(z)} + i\mathcal{E}(z) \right] \quad (1)$$

where: A_0 is a constant amplitude, $k = 2\pi/\lambda$, $\omega(z) = \omega_0 [1 + (z/z_0)^2]^{1/2}$ the beam width, $R(z) = z[1 + (z_0/z)^2]$ the radius of curvature of the wavefront and $\varepsilon(z) = \tan^{-1}(z/z_0)$ the Gouy phase retardation relative to a plane wave.

This beam is transmitted through a Kerr nonlinear optical material of length L , with a refractive index and absorption coefficient given by [2]:

$$n(I) = n_0 + \gamma I, \quad (2)$$

$$\alpha(I) = \alpha_0 + \beta I, \quad (3)$$

where: n_0 is the linear refractive index, γ the nonlinear refractive coefficient, α_0 the linear absorption coefficient and β the nonlinear absorption coefficient and I is the light intensity.

The output field for a thin local media is given by [17];

$$E_{out} = E(r, z) \exp(-\alpha_0 L / 2) (1 + q)^{(-ik\gamma/\beta - 1/2)}, \quad (4)$$

where, $q = \beta I L_{eff}$, $L_{eff} = (1 - \exp(-\alpha_0 L)) / \alpha_0$, $I_0 = |A_0|^2$ is the on-axis intensity at the waist. The irradiance distribution and phase shift of the beam at the exit surface of the sample must fulfill:

$$I_{out}(z, r) = \frac{I(z, r) \exp(-\alpha_0 L)}{1 + q(z, r)} \quad (5)$$

and

$$\Delta\phi = (k\gamma/\beta) \ln[1 + q(z, r)]. \quad (6)$$

The intensity I can be expressed, at position z , as the product of the maximum on axis value I_0 and a Gaussian local profile (G_{loc}):

$$I(r, z) = I_0 G_{loc}, \quad (7)$$

with

$$G_{loc} = \frac{\exp[-2r^2/w^2(z)]}{(1 + (z/z_0)^2)}. \quad (8)$$

In [18], it was proposed that the field after a nonlocal sample that presents solely nonlinear refraction, the photoinduced nonlinear phase change $\Delta\phi$ can be written as:

$$\Delta\phi_m(r) = \Delta\Phi_0 G_{loc}^{m/2}, \quad (9)$$

where m can be any real positive number. A value of $m = 2$ considers (local case) that the nonlinear phase changes follows the incident intensity. Other values of m (nonlocal cases) give broader ($m < 2$) or narrower ($m > 2$) nonlinear phase changes. In that paper was demonstrated that Eq. (9) describes fairly well far field intensity distributions obtained for spatial self-phase modulation and Z-scan curves.

Assuming that for a nonlocal material that presents nonlinear absorption Eq. (6) must also be fulfilled in the limit of $\beta \rightarrow 0$ Eq. (8) must be satisfied. Then it is necessary to consider that q takes the following form;

$$q_m(r) = \Delta\Psi_0 G_{loc}^{m/2}, \quad (10)$$

note that this expression is reduced to that of the local case when $m = 2$.

The field at the exit surface of the sample, under the thin sample approximation and a spatially nonlocal nonlinearity in materials that have both refractive and absorptive nonlinear responses, is given by:

$$E_{out} = E(r, z) \exp(-\alpha_0 L/2) \left[1 + \Delta\Psi_0 G_{loc}^{m/2} \right]^{(-i(\Delta\Phi_0/\Delta\Psi_0)-1/2)}. \quad (11)$$

3. Numerical results

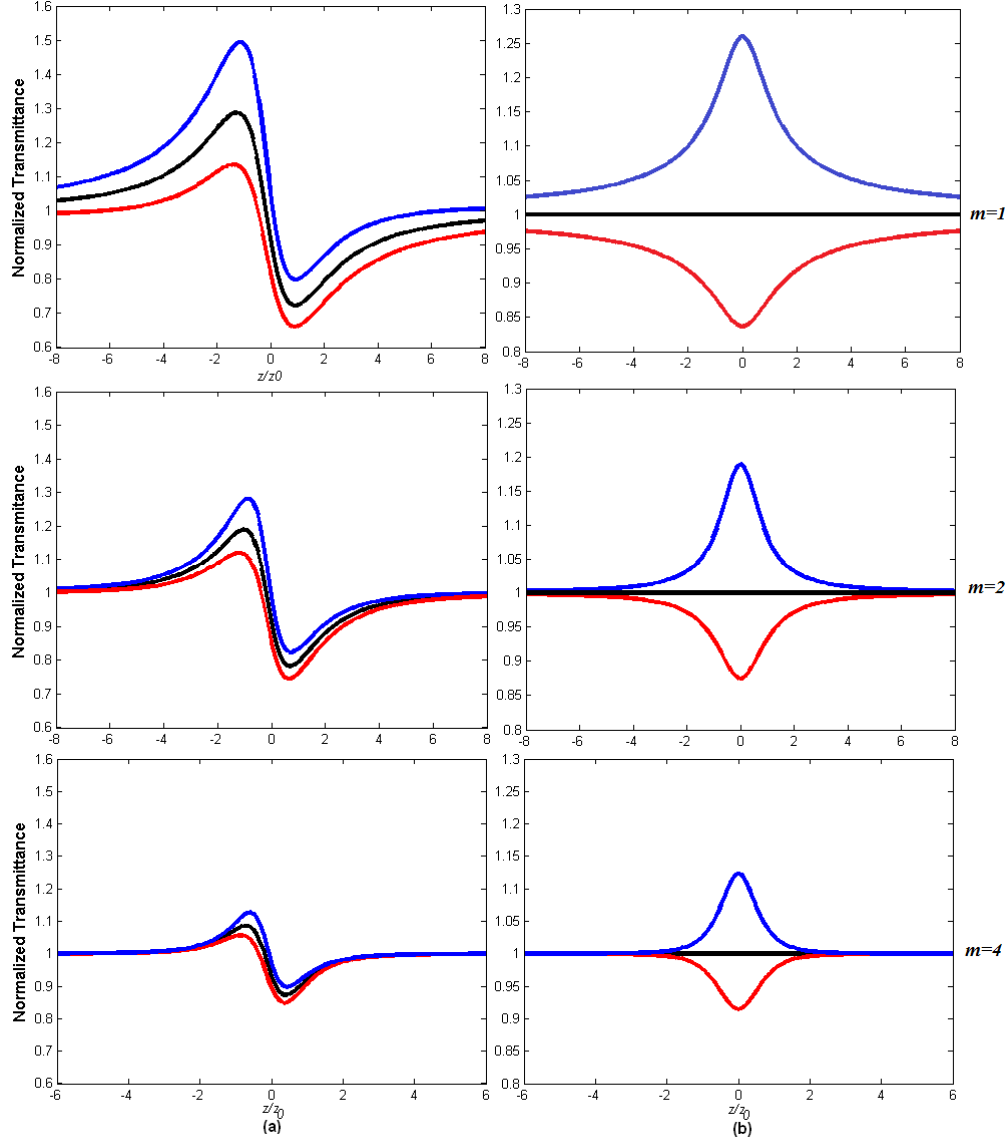


Fig. 1. Z-scan curves for closed (a) and open (b) -aperture with $\Delta\Phi_0 = -1$ rad. and $\Delta\Psi_0$ of: 0.3 (red line), 0.0 (black line) and -0.3 (blue line).

In this section the far field intensity is numerically calculated, from the Fraunhofer integral of Eq. (11), for different values of m to obtain curves for the closed- or open-aperture Z-scan cases. We consider a thin nonlinear sample (of length $L = 1 \times 10^{-3}$ m), with a linear absorption coefficient $\alpha_0 = 1 \times 10^{-1} \text{ m}^{-1}$ and illuminated with a Gaussian beam of $w_0 = 20 \text{ }\mu\text{m}$ at $\lambda = 633$

nm. Figure 1 shows the results obtained for closed (a) and open (b) -aperture Z-scan curves for different values of the m parameter, with $\Delta\Phi_0 = -1$ rad., and $\Delta\Psi_0$ values of: 0.3 (red), 0.0 (black) and -0.3 (blue). To simulate a strong nonlocality (a material where the spatial extension of the phase changes is larger than the illuminated area) we used $m = 1$, and to simulate a weak nonlocality (a material where the spatial extension of the phase changes is smaller than the illuminated area) we used $m = 4$. For the closed aperture z-scan curves we can see that the peak (valley) transmittance decreases as the parameter m increases. The same dependence is observed for the peak (valley) in the open aperture z-scan curves. The width of the peak (valley) obtained in the open aperture z-scan curves decreases as the parameter m increases.

In order to see clearly the influence of the nonlocality in the z-scan curves, in Fig. 2 we plot the closed (a) and open (b) -aperture z-scan curves using the same values of $\Delta\Phi_0 = -1$ rad., $\Delta\Psi_0 = -0.3$, with m values of: 1 (red line), 2 (black line) and 4 (blue line). Under these conditions, for the closed aperture z-scan curves, the changes in the amplitude of the peak are larger than the valley. For the open aperture z-scan curves the amplitude and width of the peak decreases as the parameter m increases.

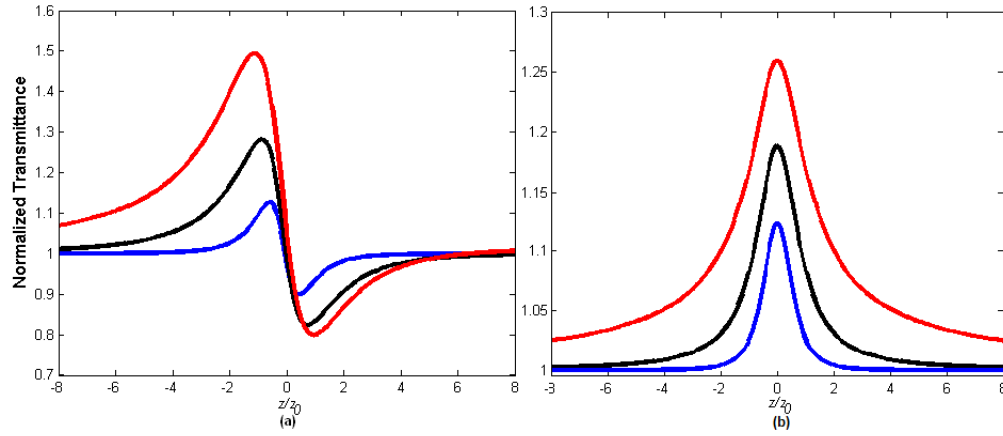


Fig. 2. Z-scan curves for closed (a) and open (b) -aperture with $\Delta\Phi_0 = -1$ rad., $\Delta\Psi_0 = -0.3$ and m of 1 (red line), 2 (black line) and 4 (blue line).

4. Analytical expressions

We use GD method in order to derive analytical expressions for the on axis far-field transmittance. According to this treatment the complex electric field at the exit plane of the sample is decomposed into a sum of Gaussian beams, with decreasing waist dimensions, through a Taylor series expansion of the photoinduced phase shift. Each individual Gaussian beam is propagated far away from the sample and finally all these beams are summed to reconstruct the far field pattern of the resulting beam at the aperture plane. The binomial series of the exiting electric field is:

$$E_{out} = E(r, z) \exp(-\alpha_0 L / 2) \sum_{n=0}^{\infty} \left[\frac{(-i\Delta\phi_0(z))^n}{n!} \times \prod_{n'=0}^n \left(1 - i(2n-1) \frac{\Delta\Psi_0}{\Delta\Phi_0} \right) \right] \exp \left[\frac{-mnr^2}{w^2(z)} \right], \quad (12)$$

the complex electric field at the aperture plane, where the Gaussian beam will be reconstructed, can be written as;

$$E_a = E(r, z) \sum_{n=0}^{\infty} \frac{[-i\Delta\phi_0(z)]^n}{n!} \prod_{n'=0}^n \left(1 - i(2n-1) \frac{\Delta\Psi_0}{\Delta\Phi_0} \right) \frac{w_{n0}}{w_n} \exp \left(\frac{-r^2}{w_n^2} - \frac{ikr^2}{2R_n} + i\theta_n \right), \quad (13)$$

where $\Delta\phi_0 = \Delta\Phi_0/[1 + (z/z_0)^2]^{m/2}$. When it is only considered the refractive response, $\Delta\Psi_0 = 0$, Eq. (13) is reduced to:

$$E_a = E(r, z) \sum_{n=0}^{\infty} \frac{[-i\Delta\phi_0(z)]^n}{n!} \frac{w_{n0}}{w_n} \exp\left(\frac{-r^2}{w_n^2} - \frac{ikr^2}{2R_n} + i\theta_n\right). \quad (14)$$

If d is the propagation distance from the sample to the aperture and $g = l + d/R(z)$, the remaining parameters of (14) are expressed as:

$$\begin{aligned} w_{n0}^2 &= \frac{w^2(z)}{mn+1} \\ d_n &= \frac{kw_{n0}^2(z)}{2} \\ w_n^2 &= w_{n0}^2 \left[g^2 + \left(\frac{d}{d_n} \right)^2 \right] \\ R_n &= d \left[1 - \frac{g}{g^2 + d^2/d_n^2} \right]^{-1} \end{aligned}$$

and

$$\theta_n = \tan^{-1} \left(\frac{d/d_n}{g} \right).$$

In order to obtain the transmittance, the on axis electric field at the aperture plane is obtained making $r = 0$ in (14). The normalized transmittance can be written as:

$$T_m(z, \Delta\phi_0) = \frac{|E(r=0, z, \Delta\phi_0)|^2}{|E(r=0, z, \Delta\phi_0=0)|^2}. \quad (15)$$

Under the far field condition $d \gg z_0$, the normalized transmittance for the N-order can be obtained numerically through the next expression:

$$T_m(z, \Delta\Phi_0) = \left| \sum_{n=0}^N \frac{1}{n!} \left[\frac{\Delta\Phi_0(z)}{(1+x^2)^{m/2}} \right]^n \frac{i^n(x+i)}{x+i(mn+1)} \right|^2, \quad (16)$$

where $x = z/z_0$. In Fig. 3, the peak–valley separation distance and peak–valley transmittance difference are plotted as functions of the m parameter for $\Delta\Phi_0 = -0.5\pi$, $-\pi$ and -4π rad. We can observe that until $\Delta\Phi_0 = -\pi$ rad., the peak–valley separation distance follows the behavior obtained for small on-axis nonlinear phase shifts. However for $\Delta\Phi_0 = -4\pi$ rad. the curve present sudden changes, for values of $m > 2.2$ the separation decreases smoothly. The peak–valley transmittance difference curves follow a similar behavior to that obtained for a small phase shift. For $\Delta\Phi_0 = -4\pi$ rad. there is a maximum of 5.9 at $m = 0.5$ and the transmittance difference decays in a fast way for larger m values. All these numerical results are consistent with that showed in [15]. The results obtained with Eq. (16) will be approximate to that obtained with the full propagation of the exit field as the N value increase. We found numerically that for phase changes of the order of π at least $N = 20$ is needed.

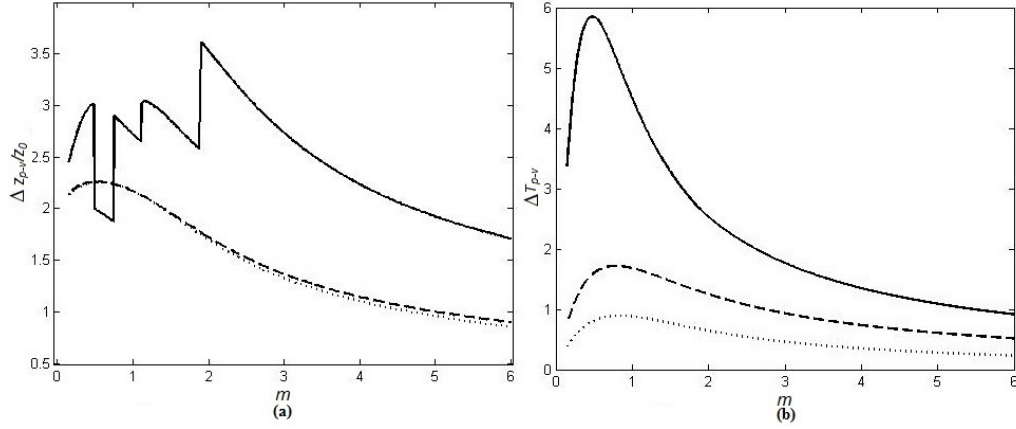


Fig. 3. Δz_{p-v} (a) and ΔT_{p-v} (b) as a function of the m obtained from evaluation of Eq. (16) with $N = 20$ and $\Delta\Phi_0 = -0.5\pi$ rad. (dotted), $\Delta\Phi_0 = -\pi$ rad. (dashed line) and $\Delta\Phi_0 = -4\pi$ rad. (solid line).

Taking into account until the second order in $\Delta\Phi_0$ of Eq. (16) we obtain the following expression for the transmittance:

$$T_m(z, \Delta\Phi_0) = 1 + \frac{2m\Delta\Phi_0 x}{[x^2 + (m+1)^2](x^2 + 1)^{m/2}} + \frac{m^2(3x^2 - (2m+1))\Delta\Phi_0^2}{[x^2 + (m+1)^2][x^2 + (2m+1)^2](x^2 + 1)^m}. \quad (17)$$

In Fig. 4 it is plotted Eq. (17) with $\Delta\Phi_0 = -0.5$ rad. for values of $m = 1, 2$ and 4 . As it can be observed with the same on-axis nonlinear phase shift the curves amplitude decrease as m increase. In Fig. 5 the peak-valley separation distance and peak-valley transmittance difference are plotted as functions of the m value for $\Delta\Phi_0$ of -0.5 rad. and -1 rad.. The Δz_{p-v} and the ΔT_{p-v} values predicted for the local case ($m = 2$) and the thermal case ($m \approx 1$) [11], are achieved when the phase change is small enough $|\Delta\Phi_0| \ll 1$ rad. When we consider $|\Delta\Phi_0|$ values of the order of 1 rad., Eq. (17) is still valid since Δz_{p-v} values decreases only slightly, however if the maximum phase change is bigger than 1 rad. it is necessary to take into account more terms in Eq. (16).

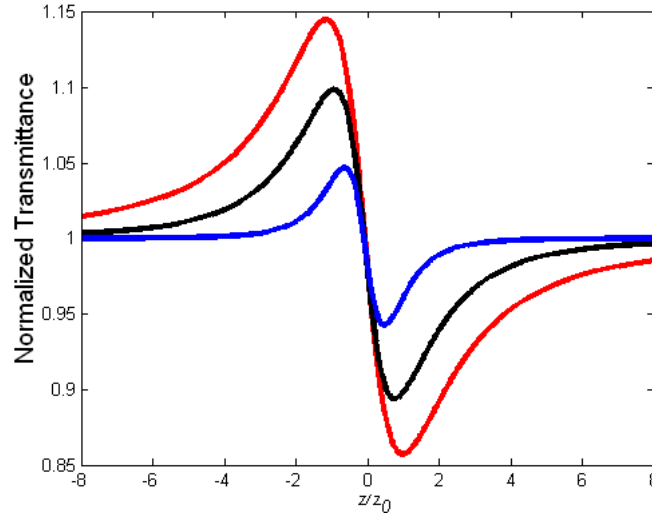


Fig. 4. Closed-aperture Z-scan curves obtained from Eq. (17) with $\Delta\Phi_0$ of -0.5 rad. and m parameter of: 1 (red line), 2 (black line) and 4 (blue line).

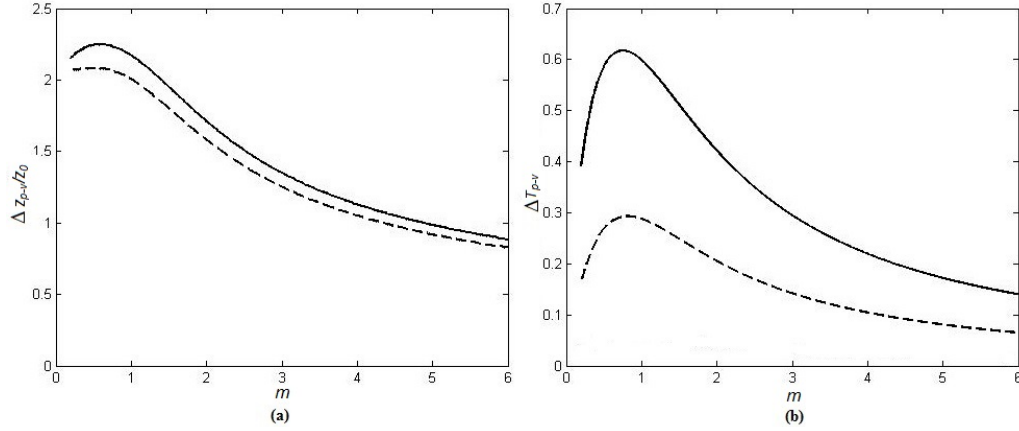


Fig. 5. Results from Eq. (17) for Δz_{p-v} (a) and ΔT_{p-v} (b) as functions of the m parameter for $\Delta\Phi_0 = -0.5$ rad. (dashed line) and $\Delta\Phi_0 = -1$ rad. (solid line).

In order to obtain simultaneously the absorptive and refractive effects we have to consider the field described in (12), to find the on axis transmittance at far field;

$$T(z, \Delta\Phi_0, \Delta\Psi_0) = 1 + \frac{2m\Delta\Phi_0 + \Delta\Psi_0(x^2 + (m+1))}{(x^2 + (m+1)^2)(x^2 + 1)}. \quad (18)$$

In Fig. 6, the Z-scan curves for a sample with $\Delta\Phi_0 = -0.1$ rad. and $\Delta\Psi_0 = -0.02$ rad. are plotted for different values of the m parameter. As can be seen, for all the m values the closed-aperture transmittance curves have lost their symmetry an effect that occurs when the absorptive nonlinearity comes to play a role.

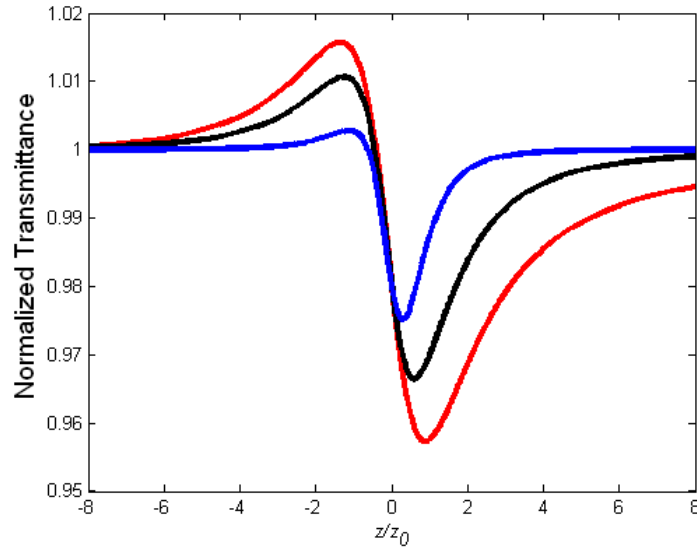


Fig. 6. Closed-aperture Z-scan curves for an on-axis nonlinear phase shift of $\Delta\Phi_0 = -0.1$ rad., $\Delta\Psi_0 = -0.02$ and m values of: 1 (red line), 2 (black line) and 4 (blue line).

The effect of decreasing the peak and enhancing the valley, in comparison of a purely refractive case, is not only due to nonlinear absorption, the nonlocal response of the sample has a similar effect.

The transmittance for the open aperture z-scan can be obtained integrating Eq. (5) [2]. In our case the following expression was obtained:

$$T_m(z, \Delta\Psi_0) = \frac{\ln[1 + q_0(z)]}{q_0(z)}, \quad (19)$$

where $q_0(z) = \Delta\Psi_0/[1 + (z/z_0)^2]^{m/2}$. Figure 7 shows the open aperture case for $\Delta\Psi_0 = 0.05$ and different values of the m parameter. In this case the amplitude of the valley is the same for all m values but the width clearly depends on the nonlocality

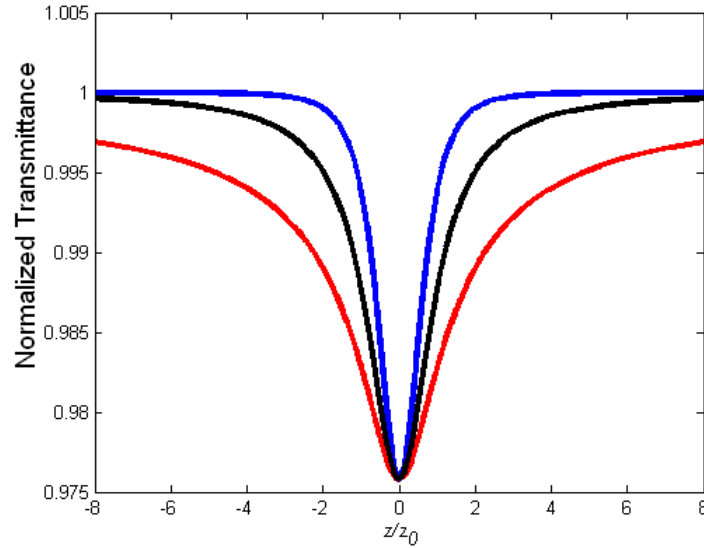


Fig. 7. Open-aperture Z-scan curves with $\Delta\Psi_0 = 0.05$ and m values of: 1 (red line), 2 (black line) and 4 (blue line).

Analytical expressions (16) and (19) can be used to fit experimental data. When the beam waist, w_0 , of the Gaussian beam is known the m parameter is the fitting parameter.

5. Experimental results fitting

Experimental z-scan curves were obtained with a green brilliant sample ($C_{27}H_{34}N_2O_4S$) [19]. CW illumination from a helium neon laser at 633nm was used, the laser beam was focused by a convergent lens of 3.5 cm of focal length getting a beam waist of $18\mu m$. The sample was deposited in a 1 mm width quartz cell and moved on axis direction around the lens focus by a computer-controlled servo motor. The transmitted light was measured; through on axis small aperture (1 mm radius) at far field located 1 m away of the lens, or without aperture by a photo-detector, as function of the sample position to obtain the closed- or open-aperture z-scan curves. In Fig. 8 experimental and numerical results for the closed- and open-aperture Z-scan curves are showed for laser powers of: 1 mW (*), 3 mW (o) and 5 mW (+). The closed-aperture Z-scan curves are asymmetric, exhibit a negative nonlinear refractive index and the amplitude of the Z-scan curves grew with the incident power. The Δz_{p-v} value range from 3 mm to 3.3 mm (2 to 2.1 z_0), and ΔT_{p-v} values are ranging from 0.2 to 0.9. The open-aperture curves are also asymmetric, exhibit a negative nonlinear absorption coefficient and the amplitude of the curves are ranging from 0.04 to 0.07. The numerically calculated Z-scan curves with Eqs. (15) and (18), are shown in continuous lines with $m = 0.9$ and $\Delta\Phi_0$ of: -0.12π rad. for 1 mW, -0.4π rad. for 3 mW and -0.6π rad. for 5mW curve in the closed-aperture case. For the open-aperture case $\Delta\Psi_0$ is: -0.09 for 1mW, -0.105 for 3mW and -0.12 for 5mW. From the previous results we can say that the nonlinearity exhibited by the sample

was negative of thermal type. The nonlinear absorption coefficient, β , was negative with a magnitude of the order of -0.038 cm/W that depended on the incident power, but the difference was not large.

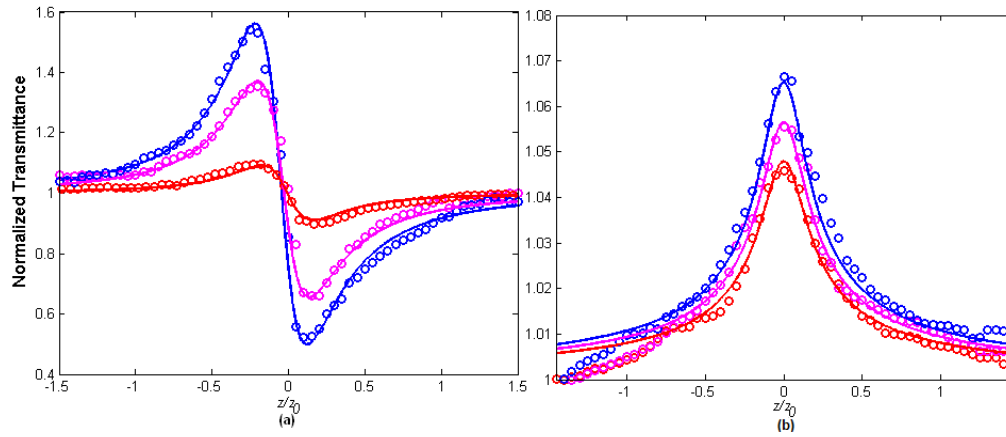


Fig. 8. Experimental (symbol) and numerical (lines), a) closed- and b) open-aperture Z-scan curves for incident power of: 1 mW(red), 3 mW(magenta) and 5 mW(blue).

6. Conclusions

An extension of the nonlocal model for materials with simultaneous nonlinear refractive and absorptive contributions was described. Two simple expressions for the on axis intensity (closed aperture) and total transmitted power (open) were derived following the Gaussian decomposition method for any magnitude of the nonlinear contributions. Evaluation of the formulas for different cases was presented. Experimental results of a sample that presents both nonlinear refraction and absorption were obtained for the closed- and open-aperture Z-scan. The experimental results were fitted with a nonlocal parameter $m = 0.9$, obtaining excellent agreement between theory and experiment.